Indian Journal of Biochemistry & Biophysics
Vol. 58, August 2021, pp. 373-380

# Biofabrication of Silver Oxide Nanoparticles (SO-NP) by autolysate of *Pseudomonas mendocina* PM1, and assessment of its antimicrobial/antibiofilm potential

Venkatesh Chaturvedi[1]*, Piyoosh Kumar Babele[2, 3] & Prabhakar Singh[4]

[1]School of Biotechnology, Banaras Hindu University, Varanasi-221 005, Uttar Pradesh, India

[2]Chemical & Biomolecular Engineering, Vanderbilt University, Nashville, Tennessee-37235, USA

[3]College of Agriculture, Rani Lakshmi Bai Central Agricultural University, Jhansi-284 003, Uttar Pradesh, India

[4]Department of Anatomy (Electron Microscopy Facility), All India Institute of Medical Sciences, New Delhi-110 029, Delhi, India

*Received 06 February 2021*; *revised 12 March 2021*

Silver oxide Nanoparticles (SO-NP) exhibit excellent light absorbing, semi conducting properties and hence are employed in a wide range of applications such as catalyst, biosensors, and in fuel cells. Green synthesis of nanoparticles using different microorganisms is widely accepted since this method is in expensive and eco-friendly. Nanoparticles synthesized by this route are smaller in size, highly stable, show high reactivity and stability. In this context, biofabrication of Silver Oxide Nanoparticles (SO-NP) by autolysate of *Pseudomonas mendocina* PM1 has been evaluated. Synthesis of SO-NP was observed, when autolysate of *P. mendocina* PM1 was incubated with 0.5 mM $AgNO_3$ in dark for 24 h. Synthesis of SO-NP was confirmed by UV-Vis analysis. SO-NP was further confirmed by Transmission Electron Microscopy (TEM) and X-ray Diffraction (XRD) which confirmed presence of SO-NP. XRD revealed that SO-NP were of the type $Ag_3O_4$. FTIR analysis indicated that peptides were involved in the reduction and stability of SO-NP. SO-NP's showed potent anti-microbial/ anti-biofilm activity against common pathogenic/non-pathogenic bacteria. This is the first report of synthesis of SO-NP by *P. mendocina* PM1.

**Keywords**: *Acalypha indica*, *Glycine max*, *Pseudomonas aeruginosa*, *Pseudomonas mendocina* PM1, *Rhodobacter sphaeroides*

Metallic silver has been considered as a therapeutic agent since ages. Silver has been employed in control of a wide variety of ailments such as wound healing, burns, mental illness, and epilepsy[1]. Silver is also considered as a potent antibacterial and antifungal agent and is widely used for the control of various pathogenic fungi and bacteria. Major drawback of silver ions is that they tend to precipitate easily and hence cannot be employed as antimicrobial agent[2]. Recently, with emergence of nano technology, use of silver nanoparticles instead of metallic silver has been conceived as a healthier alternative due to its small size and ease of handling[3]. Nanoparticles are defined as solid particles having size ranging from 1-100 nm. These particles may exist as such or in form of a suspension[4]. Among different classes of nanoparticles available, Metallic Nanoparticles most commonly Silver Nanoparticles (SNP's) due to their small size, large surface area and high reactivity has led to its widespread use in various nanotechnology-based products[5]. Synthesis of SNP's is usually achieved by reduction of concerned metal salts by employing chemical methods such as application of strong reducing agents such as sodium borohydride[6], and hydrazine[7], physical methods involving radiation based reduction of silver ions by either γ-rays[8], microwave[9] or ultrasound[10]. Most of these processes are either costly and also not ecofriendly[11]. Often, chemicals employed in synthesis are difficult to separate therefore nanoparticles synthesized by this route cannot be employed in biological systems[12]. Therefore, green synthesis of SNP's by employing various bacterial/fungal strains and plant extracts has been proposed[13,14]. These methods are cheap, efficient and do not have adverse effects on environment. There are many reports of biomimetic synthesis of SNP' using various plant extracts, *viz.* Tea[15], *Cinnamon zeylanicum*[16], *Azadirachta indica*[17], *Glycine max*[18],

*Correspondence:
Phone: 91-0542-2368331;
Fax No: 91-0542-2369693
E-mail: venkatesh_chaturvedi@bhu.ac.in

*Acalypha indica*[19]. Synthesis of SNP's by employing plant extracts is a fast process, wherein, the synthesis is achieved within few hours after addition of silver nitrate. A major drawback of this process is that the size of nanoparticles is usually large (50-200 nm), they are unstable and show aggregation/anisotropy due to high concentration of reducing agents[17]. Another route of green synthesis of SNP's is through bacterial and fungal strains where SNP's are synthesized either inside the cell (intracellular) or outside the cell (extra cellular)[20]. SNP's have been synthesized from different bacterial/fungal strains, such as *Bacillus cereus*[21], *Escherichia coli*[14], *Staphylococcus aureus*[22], *Fusarium oxysporum*[11], *Aspergillus niger*[12,23]. Extracellular synthesis of nanoparticles by employing autolysate of bacterial/ fungal cell is considered as a preferable method since the synthesis occurs by autolysate in absence of cells and there is no need for separation of SNP's from bacterial and fungal biomass[24]. Reports have shown that SNP's synthesized from this route are smaller in size and show reduced aggregation since concentration of reducing agents in autolysates are usually lower as compared to plant extracts. Literature survey suggests that size of nanoparticles is the major factor that governs its reactivity. Generally, small sized nanoparticles (1-20 nm) are better suited for antimicrobial purposes[5]. Silver Oxide Nanoparticles (SO-NP) belong to the class of SNP, and are basically metal oxides where silver exist in multivalent state such as $Ag_2O$, AgO, $Ag_3O_4$ and $Ag_2O_3$[25]. SO-NP's exhibits excellent semiconductor properties. Photo activation of silver oxides lead to surface enhanced Raman Scattering (SERS) and hence, these are widely used in application such as nano-electronics, biological devices such as biosensors, *etc*[26]. Recent reports have demonstrated that SO-NP's exhibit anti-microbial properties[27]. SO-NP's are generally prepared by chemical/ electrochemical techniques[28]. Recently, green synthesis of SO-NP's using extracts of different bacterial and fungal strains have been proposed[26,27,29]. In this investigation, green synthesis of SO-NP's by a strain of *Pseudomonas mendocina* PM1 has been presented. This bacterium was isolated from a detergent contaminated pond situated in Varanasi city, India[30]. *P. mendocina* is an environmental bacterium which has been implicated in bioremediation of different xenobiotic compounds, such as Toluene[31], and Sodium Dodecyl Sulfate (SDS)[30]. Its role in synthesis of nanoparticles especially SO-NP's has not been evaluated. This study concentrates on synthesis of SO-NP by employing autolysate of *P. mendocina*. SO-NP's were characterized by UV-Vis spectroscopy, Transmission Electron Microscopy (TEM), X-ray Diffraction (XRD) analysis. The mechanism behind SO-NP formation was evaluated by FTIR analysis. SO-NP synthesized by this method showed excellent anti-microbial activity against common pathogenic bacteria. Further, SO-NP also inhibited biofilm formation in *Bacillus subtilis* MTCC 441.

## Materials and Methods

### Strains, Culture medium and growth conditions

*Pseudomonas mendocina* strain PM1 (Genbank Accession No. HM627520) was isolated from a detergent contaminated pond situated at a place called Pisach Mochan in Varanasi city, India[30]. This strain was employed for synthesis of SO-NP's. *Bacillus subtilis* MTCC 441, and *Staphylococcus aeurus* MTCC 737 were obtained from IMTECH Chandigarh, India. For synthesis of SO-NP's, strain PM1 was grown in LB medium, which contained the following (g/L): tryptone; 10.0, yeast extract; 5.0; NaCl, 10.0; pH-7.0. A single colony of strain PM1 was inoculated in 500 mL LB medium and incubated at 120 rpm at 30°C in a rotatory shaker. After growth, cells were separated by centrifugation at 10,000 rpm for 15 min. The cell pellet was washed thrice with 50 mL MQ water and final cell pellet was used for synthesis of SO-NP's.

### Synthesis of SO-NP's

In this study, extracellular or autolysate mediated synthesis of SO-NP's was performed. For preparation of autolysate, 2 g (fresh weight) cell biomass was suspended in 100 mL MQ water and incubated at 120 rpm at 30°C for 48 h. After incubation, the suspension was centrifuged at 10,000 rpm for 15 min. The supernatant was filtered through Whatman filter paper no. 1. The autolysate was mixed with 100 mL 1 mM silver nitrate solution and incubated in dark at 120 rpm at 30°C. At regular time intervals, 2 mL solution was withdrawn and synthesis of SO-NP's was monitored by UV-Vis spectroscopy using Shimadzu UV-Vis spectrophotometer (UV-1800). Autolysate mixed with equal volume of MQ water, was employed as a positive control.

### Characterization of SO-NP's

The particle size and distribution of SO-NP's was determined by TEM analysis. For TEM analysis, a drop of autolysate containing SO-NP's was employed. TEM was performed using Morgagni 268D (Fei Electron Optics). The presence of SO-NP's was

further confirmed by XRD analysis. The autolysate containing silver nitrate was evaporated at 60°C in a hot air oven. The dried mass was scrapped with the help of a needle and resulting fine powder was used for XRD analysis. Ethanol washed, completely dried powder of SO-NPs was used for the X-ray diffraction analysis (XRD). The spectra were recorded in Rigaku Miniflex II X-ray diffractometer (Rigaku Co., Ltd., Japan) operated at 30 kV, 15 mA. The diffraction was recorded at 2θ angles from 20 to 80°.

**FTIR analysis of autolysate and SO-NP's**

To study the mechanism behind synthesis of SO-NP by strain PM1, FTIR analysis of autolysate and autolysate containing silver nitrate was performed. Autolysate and autolysate containing 0.5 mM silver nitrate (10 mL each) was evaporated to dryness at 60°C in a hot air oven. The resulting dry mass was used for FTIR analysis. The powder of dried autolysate and SO-NP's was mixed with potassium bromide (1:100) and FTIR spectra were recorded in a Perkin Elmer infrared spectrophotometer (Perkin Elmer Inc., Waltham, MA, USA).

**Microbial toxicity of SO-NP's**

Microbial toxicity of SO-NP was evaluated by disc diffusion assay and MIC estimation following growth in LB medium containing different concentrations of SO-NP's. The bacterial strains employed in this study were, *B. subtilis* MTCC 441, *Staphylococcus aeurus* MTCC 737, *P. aeruginosa* strain N1[30], and *E. coli* JM109. A single colony of each the strains was inoculated in 10 mL LB medium and incubated at 120 rpm at 30°C. After overnight incubation, 100 µL cultures each were spread on the surface of nutrient agar plate. After spreading five sterile filter paper discs were placed on the surface of nutrient agar plates in a circular fashion. A stock solution of SO-NP was prepared by suspending 5 mg of SO-NP in 1 mL of MQ water. SO-NP was suspended by sonication for 2 min. Different concentrations of SO-NP from stock solution (2.5, 5.0, 7.5, and 10 µg) was placed on each filter paper disc and anti- microbial activity was accessed by formation of inhibitory zone.

**Anti-biofilm activity of SO-NP's**

Biofilm formation was studied microscopically after staining the attached cells with crystal violet. *B. subtilis* MTCC 441 was grown for overnight in LB medium. After proper growth, the OD at 600 nm was set 1.0 by dilution with fresh LB medium. 100 µL was inoculated in 10 mL LB medium. In control tube, only LB medium was taken. In test, SO-NP at a concentration of 5 and 10 µg/mL was supplemented in LB medium. For biofilm growth, autoclaved glass slide were inserted into the test tubes and the tubes were placed in a BOD incubator at 37°C. After 5 h, slides where removed and washed twice with phosphate buffer to remove loosely bound cells. The slides where then put in 5% glutaraldehyde in phosphate buffer for 12 h for fixation. After fixation the slides where washed twice with phosphate buffer and stained in 1% crystal violet for 20 min. The slide where washed twice with phosphate buffer, air dried and visualized under microscope (Nikon Eclipse 200) under 40X magnification.

## Results and Discussion

**Synthesis of SO-NP's**

After addition of silver nitrate to autolysate, a change of color from colorless to slight yellow was observed after 1 h of incubation. With time, this color gradually deepened to light brown (6 h) and then to dark brown (12 h). After 24 h of incubation, the color of the solution became constant and no further change was observed (Fig 1A). The change in color can be attributed to excitation of surface plasmon vibrations of Ag nanoparticles. The color change was monitored by UV-visible spectroscopy,

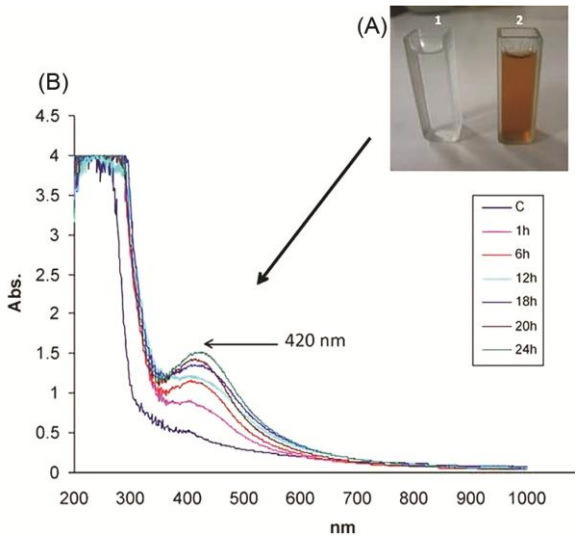


Fig.1 — Synthesis of SO-NP's (A) Visible color change in autolysate of *P. mendocina* PM1 after addition of 0.5 mM AgNO3, after 24 h of incubation; and (B) UV-Vis spectrum of autolysate containing 0.5 mM AgNO3 after different time intervals

by recording absorption spectrum in the range of 200-1000 nm (Fig. 1B). It is clear from the figure that the color change arising after addition of silver nitrate corresponds to appearance of a peak at 420 nm. This peak gradually intensified with time. These results are accordance with previous report of Bai *et al*.[32], where SNP's synthesized from cell filterate of *Rhodobacter sphaeroides* showed appearance of a peak at 420 nm, corresponding to surface plasmon absorption band of SNP. Dhoondia and Chakrborty[33] have reported that SO-NP synthesized by *Lactobacillus mindensis* shows a peak at 430 nm.

**TEM analysis of SO-NP's**

Figure 2A & B, represents TEM images of SO-NP. It is clear from these figures that nearly spherical and mono dispersed SO-NP were formed. Also, no aggregation between nanoparticles was observed. From TEM images particle size and its distribution was calculated. The results are depicted in (Fig. 3). It was observed that majority of nanoparticles (43%) were in the range of 10-20 nm, 24% were in the range of 5-10 nm and 21% were in the range of 20-30 nm. These results clearly represent that size distribution of nanoparticles fall under 5-30 nm, with major portion under 10-20 nm range. These results also show that there is less anisotropy between nanoparticles. Our results are in accordance with Dhoondia and Chakrborty[33], where SO-NP in the range of 2-20 nm was synthesized by *Lactobacillus mindensis.* Results of this study show that nanoparticles synthesized by *P. mendocina* are smaller as reported by other workers, *Brevibacterium casei* (10-50 nm)[34], *Phaenerochaete chrysosporium* (50-200 nm)[35], *Bacillus licheniformis* (50 nm)[36], *E. coli* (50 nm)[14], *Corynebacterium glutamicum* (5-50 nm)[37]. These results clearly indicate that *P. mendocina* has the potential to synthesize small sized SO-NP's.

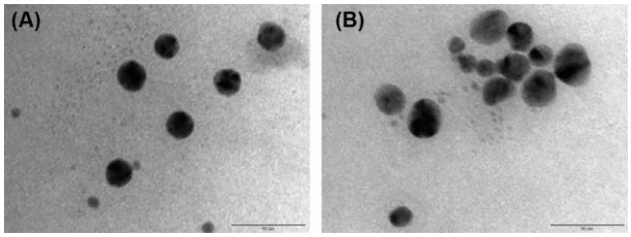


Fig. 2 — TEM image of SO-NP's

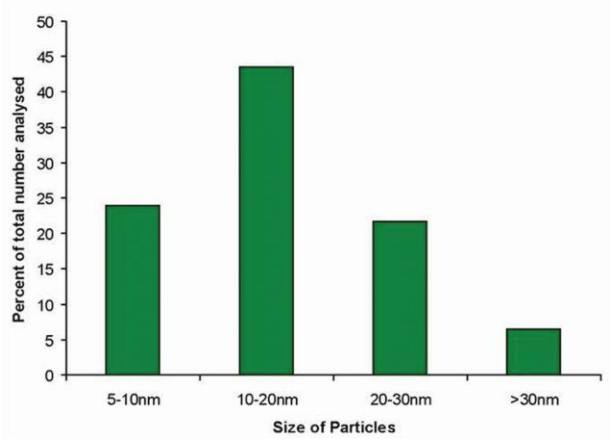


Fig. 3 — Size distribution of SO-NP's

**XRD analysis of SO-NP's**

The oven dried samples of SO-NPs (silver oxide nanoparticles) were subjected to X-ray diffraction (XRD) analysis and the crystalline nature of silver nanoparticles was predicted. XRD spectrum of SO-NPs clearly showed that the pure SO-NPs were indeed formed after reaction with cell extract. From the XRD data in (Fig. 4), clearly represented that all of the peaks match well with the Bragg reflections of the standard monoclinic ($Ag_3O_4$; JC PDF401054; a=3.5787, b=9.2079, c=5.6771, which corresponded to silver oxide nanoparticles. All the reflected peaks in this pattern were found to match with JCPDF of $Ag_3O_4$ showing 2θ values (120) (031) (022) and (221)[25].

**FTIR analysis of autolysate and autolysate containing silver nitrate**

FTIR absorption spectra provide the possible interaction between the silver nitrate and the compound responsible for the reduction of silver ions and stabilization of Ag nanoparticles. In this investigation sharp FTIR absorption peaks were found at 1109.28 $cm^{-1}$, 1385.14 $cm^{-1}$, 1660.38 $cm^{-1}$,

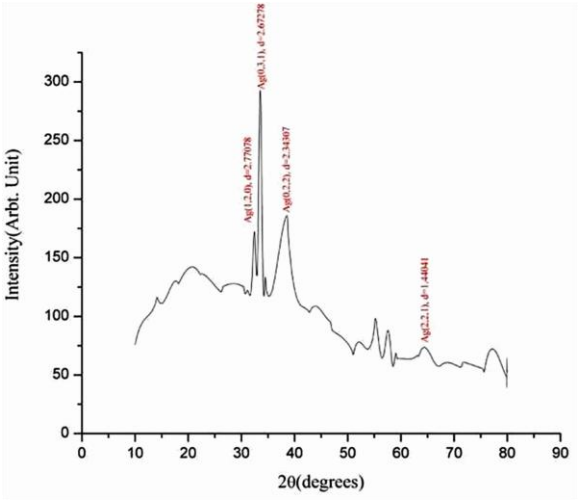


Fig. 4 — XRD spectrum of SO-NP's

2924.70 $cm^{-1}$ and 3418.33 $cm^{-1}$ in the autolysate of *P. mendocina.* But in case of autolysate reduced Ag the absorption peaks were observed at 1092.37 $cm^{-1}$, 1384.12 $cm^{-1}$, 1639.95 $cm^{-1}$, 2926.11 $cm^{-1}$, and 3438.27 $cm^{-1}$. The band at 3418.33 $cm^{-1}$ in autolysate and the 3438.27 $cm^{-1}$ in autolysate reduced Ag appeared due to stretching vibration of -N-H- of primary amines. Whereas, peak at 2924.70 $cm^{-1}$ and 2926.11 $cm^{-1}$ in autolysate and autolysate reduced Ag revealed the stretching vibration of -N-H- of secondary amines. The stretching vibration of -N-H- explained that proteins/peptides/free amino acids were present in the autolysate. The peak found at 1660.38 $cm^{-1}$ in autolysate was shifted to 1639.5 $cm^{-1}$ after reduction and a new peak appeared at 1563.4 $cm^{-1}$ in autolysate reduced Ag. The wave number of 1660.38 and 1563.4 were assigned to stretching vibration of -C=C- and the shifted peak at 1639.95 $cm^{-1}$ was assigned to the stretching of -C=O- of aromatic compounds. The band at 1385.14 $cm^{-1}$ and 1384.62 $cm^{-1}$ in autolysate and autolysate reduced Ag corresponds to -N-O- stretching of nitro compounds and also the peak at 1384.62 $cm^{-1}$ became sharpen and strong. The peak at 1109.28 $cm^{-1}$ in autolysate was shifted to 1092.37 $cm^{-1}$ after reduction, which corresponds to the stretching vibration of-C-O- of some ester compounds (Fig. 5). The overall results explained that proteins, aromatic compounds and some ester compounds present in the cell autolysate were responsible for reduction of silver and stabilization of SO-NP's. Role of bacterial peptides and aromatic compounds in formation of SNP's has been demonstrated by a number of worker's[14,20,21,32] and our results are consistent with these findings.

**Microbial toxicity of SO-NP's**

Anti-microbial effect of SO-NP on different bacterial strains was evaluated by disc diffusion assay and by estimating Minimal Inhibitory Concentration (MIC) following growth in liquid medium supplemented with different concentrations of SO-NP's. For disc diffusion assay, SO-NP, at a

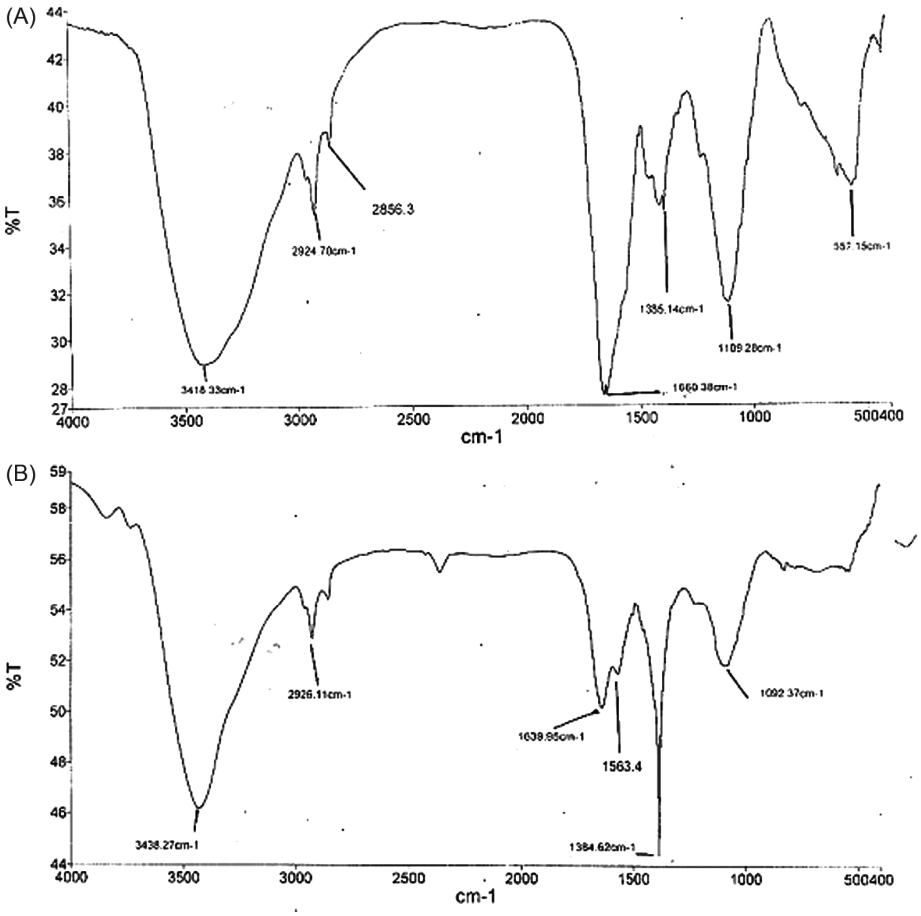


Fig. 5 — FTIR spectrum of (A) Autolysate of strain PM1; and (B) Autolysate containing 0.5 mM AgNO3

concentration of 2.5, 5.0, 7.5, and 10 µg were employed. Appearance of inhibitory zone was observed at 2.5 µg concentrations in all the isolates and diameter of inhibitory zone increased with increasing concentration of SO-NP and largest zone was observed at 10 µg concentrations. Therefore, diameter of inhibitory zone was calculated at this concentration. The results are depicted in (Fig. 6 & Table 1). It is clear from the results that SO-NP's possess anti-microbial activity against tested bacterial isolates. It is clear from the results that SO-NP's were more toxic to Gram negative bacteria such as *E. coli* and *P. aeruginosa*, when compared with Gram positive bacteria such as *B. subtilis* and *S. aeurus.* These differences in toxicity of SO-NP's can be attributed to the differences in structure of cell membranes of Gram positive and negative bacteria. Gram positive bacteria possess a thick peptidoglycan layer, which inhibits entry of SNP's inside the bacterium[4,22]. Findings of this study that SO-NP's are toxic to bacterial strains are consistent with recent findings which clearly suggest that SO-NP's belonging to $Ag_2O$ group are toxic to bacteria[25-27].

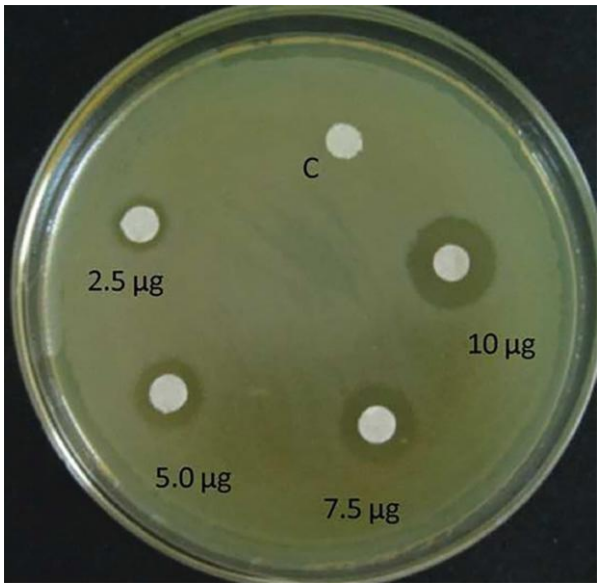


Fig. 6 — Representative figure showing anti-microbial activity of SO-NP's against *P. aeruginosa* N1

Table 1 — Anti-microbial activity of SO-NP's

| Bacterial strains | Diameter zone Inhibitory of (mm) | MIC (µg/mL) |
|---|---|---|
| *E. coli* JM109 | 20±1 | 8 |
| *P. aeruginosa* N1 | 17±0.7 | 12 |
| *B. subtilis* MTCC 441 | 16±0.8 | 15 |
| *S. aeurus* MTCC 737 | 14±0.5 | 20 |

**Anti-biofilm activity of SO-NP's against *B. subtilis* MTCC 441**

Biofilms can be defined as complex bacterial communities in which the bacterial cell form a layer like structure, which is held together by a covering of an extracellular matrix[38]. The main component of this matrix is exopolysaccharides (EPS), (secreted by the bacterium), proteins, and nucleic acids. Biofilms offer protection to growing bacteria from external stresses such as heat, desiccation and presence of antibiotics/antimicrobials by acting as a protective covering and by inhibiting entry of antimicrobials inside the biofilms. Therefore, biofilms are one of the major causes of persistent infections and are considered as a serious medical problem[39]. In recent years, there has been a tremendous thrust in identification novel molecules/metabolites that show anti-biofilm activity. *B. subtilis* is considered as a model organism for the study of biofilm development and detailed mechanism of biofilm formation has been evaluated[40]. Biofilm formation occurs in three distinct stages; attachment of bacteria to abiotic surface, multiplication of bacteria leading to formation of a group of cells called micro colonies and in the last stage micro colonies grow and form mature biofilms. Microcolony formation is considered as a crucial step in biofilm formation[41]. In this study, effect of SO-NP on microcolony formation in *B. subtilis* MTCC 441 has been evaluated. MIC for SO-NP in *B. subtilis* was 15 µg/mL. Therefore, biofilm formation was studied below this concentration. In control (Fig 7A), micro colonies are clearly evident and are represented by small group of cells attached to glass surface. However, in presence of different concentration of SO-NP, a clear dose dependent reduction in micro-colony formation was observed. At a concentration of 5 µg/mL, bacteria were attached to glass surface but no

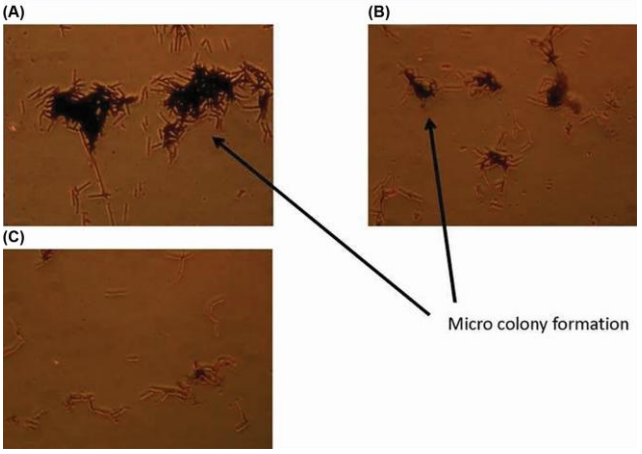


Fig. 7 — Anti biofilm activity of So-NP's against *B. subtilis* MTCC 441. (A) Control; (B) 5 µg/mL SO-NP's; and (C) 10 µg

microcolony formation was observed (Fig. 7B). At a concentration of 10 µg/mL, further reduction in number of bacteria attached to glass surface was observed (Fig. 7C). These results confirm that SO-NP's possess potent anti-biofilm potential.

## Conclusion

In the present study, green synthesis of spherical, monoclinic SO-NP using autolysate of *P. mendocina* has been presented. The size of SO-NP was in the range of 5-30 nm and was small as reported by other workers. XRD analysis showed that the state of silver in SO-NP's was $Ag_3O_4$. SO-NP's showed excellent anti-microbial properties against pathogenic and non-pathogenic bacteria. SO-NP's also showed anti-biofilm activity against *B. subtilis*. It can be concluded that autolysate of *P. mendocina* PM1 can be employed for synthesis of SO-NP.

## Acknowledgement

VC is grateful to IOE BHU for the Start-up Grant.

## Conflict of interest

All authors declare no conflict of interest.

## References

1 Palomero EO, Cunningham AL, Davies BW & Jones RA, Antibacterial thiamine inspired silver (I) and gold (I) N-heterocyclic carbene compounds. *Inorganica Chim Acta*, 517 (2021) 120152.

2 Alahmad A, Feldhoff A, Bigall NC, Rusch P, Scheper T & Walter JG, *Hypericum perforatum* L.-mediated green synthesis of silver nanoparticles exhibiting antioxidant and anticancer activities. *Nanomaterials (Basel)*, 11 (2021) 487.

3 Kim KJ, Sung WS, Moon SK, Choi JS, Kim JG & Lee DG, Antifungal effect of silver nanoparticles on dermatophytes. *J Microbiol Biotechnol*, 18 (2008) 1482.

4 Znak Z, Zin O, Mashtaler A, Korniy S, Sukhatskiy Y, Gogate PR, Mnykh R & Thanekar P, Improved modification of clinoptilolite with silver using ultrasonic radiation. *Ultrason Sonochem*, 73 (2021) 105496.

5 Rai M, Yadav A & Gade A, Silver nanoparticles as a new generation of antimicrobials. *Biotechnol Adv*, 27 (2009) 76.

6 Zhang ZQ, Patel RC, Kothari R, Johnson CP, Friberg SE & Aikens PA, Stable silver clusters and nanoparticles prepared in polyacrylate and inverse micellar solutions. *J Phys Chem B*, 104 (2000) 1176.

7 Taleb A, Petit, C & Pileni MP, Synthesis of Highly Monodisperse Silver Nanoparticles from AOT Reverse Micelles: A Way to 2D and 3D Self-Organization. *Chem Mater*, 9 (1997) 950.

8 Henglein A & Giersig M, Formation of colloidal silver nanoparticles: Capping action of citrate. *J Phys Chem B*, 103 (1999) 9533.

9 Gao F, Lu QY & Komarneni S, Interface reaction for the self-assembly of silver nanocrystals under microwave-assisted solvothermal conditions. *Chem Mater*, 17 (2005) 856.

10 Pietro PD, Strano G, Zuccarello L, & Satriano C, Gold and silver nanoparticles for applications in theranostics. *Curr Top Med Chem*, 16 (2016) 3069.

11 Duran N, Priscyla D, Marcato PD, Alves O, De Souza G & Esposito E, Mechanistic aspects of biosynthesis of silver nanoparticles by several *Fusarium oxysporum* strains. *J Nanobiotechnology*, 3 (2005) 1.

12 Gade AK, Bonde P, Ingle AP, Marcato PD, Duran N & Rai MK, Exploitation of *Aspergillus niger* for synthesis of silver nanoparticles. *J Biobase Mater Bioenergy*, 2 (2008) 243.

13 Mukherjee P, Roy M, Mandal BP, Dey GK, Mukherjee PK, Ghatak J, Tyagi AK & Kale SP, Green synthesis of highly stabilized nanocrystalline silver particles by a non-pathogenic and agriculturally important fungus *T. asperellum*. *Nanotechnology*, 19 (2008) 075103

14 Gurunathan S, Kalishwaralal K, Vaidyanathan R, Venkataraman D, Pandian SR, Muniyandi J, Hariharan N & Eom SH, Biosynthesis, purification and characterization of silver nanoparticles using *Escherichia coli*. *Colloids Surf B Biointerfaces*, 74 (2009) 328.

15 Begum NA, Mondal S, Basu S, Laskar RA & Mandal D, Biogenic synthesis of Au and Ag nanoparticles using aqueous solutions of black tea leaf extracts. *Colloids Surf B Biointerfaces*, 71 (2009) 113.

16 Sathishkumar M, Sneha K, Won SW, Cho CW, Kim S & Yun YS, *Cinnamon zeylanicum* bark extract and powder mediated green synthesis of nano-crystalline silver particles and its bactericidal activity. *Colloids Surf B Biointerfaces*, 73 (2009) 332.

17 Tripathi A, Chandrasekaran N, Raichur AM & Mukherjee A, Antibacterial applications of silver nanoparticles synthesized by aqueous extract of *Azadirachta indica* (Neem) leaves. *J Biomed Nanotechnol*, 5 (2009) 93.

18 Vivekanandhan S, Misra M & Mohanty AK, Biological synthesis of silver nanoparticles using Glycine max (soybean) leaf extract: an investigation on different soybean varieties. *J Nanosci Nanotechnol*, 9 (2009) 6828.

19 Krishnaraj C, Jagan EG, Rajasekar S, Selvakumar P, Kalaichelvan PT & Mohan N, Synthesis of silver nanoparticles using Acalypha indica leaf extracts and its antibacterial activity against water borne pathogens. *Colloids Surf B Biointerfaces*, 76 (2010) 50.

20 Basavaraja S, Balaji S, Lagashety A, Rajasab A & Venkataraman A, Extracellular biosynthesis of silver nanoparticles using the fungus *Fusarium semitectum*. *Mater Res Bull*, 43 (2008) 1164.

21 Ganesh Babu MM & Gunasekaran P, Production and structural characterization of crystalline silver nanoparticles from *Bacillus cereus* isolate. *Colloids Surf B Biointerfaces*, 74 (2009) 191.

22 Nanda A & Saravanan M, Biosynthesis of silver nanoparticles from *Staphylococcus aureus* and its antimicrobial activity against MRSA and MRSE. *Nanomedicine*, 5 (2009) 452.

23 Jain N, Bhargava A, Majumdar S, Tarafdar JC & Panwar J, Extracellular biosynthesis and characterization of silver nanoparticles using *Aspergillus flavus* NJP08: a mechanism perspective. *Nanoscale*, 3 (2011) 635.

24 Saifuddin N, Wong C & Yasumira A, Rapid biosynthesis of silver nanoparticles using culture supernatant of bacteria with microwave irradiation. *J Chem*, 6 (2009) 61.

25 Rahman MM, Khan SB, Asiri AM, Alamry KA & Al-Youbi AO, Effect of particle size on the photocatalytic activity and sensing properties of CeO2 nanoparticles. Int. *J Electrochem Sci*, 8 (2013) 323.
26 Boopathi S, Gopinath S, Boopathi T, Balamurugan V, Rajeshkumar R & Sundararaman M, Characterization and antimicrobial properties of silver and silver oxide nanoparticles synthesized by cell-free extract of a mangrove-associated *Pseudomonas aeruginosa* M6 using two different thermal treatments. *Ind Eng Chem Res*, 51 (2012) 5976.
27 Allahverdiyev AM, Abamor ES, Bagirova M & Rafailovich M, Antimicrobial effects of TiO(2) and Ag(2)O nanoparticles against drug-resistant bacteria and leishmania parasites. *Future Microbiol*, 6 (2011) 933.
28 Wei W, Mao X, Ortiz LA, & Sadoway DR, Oriented silver oxidenano structure synthesized through a template-free electrochemical route. *J Mater Chem*, 21 (2011) 432.
29 Thenmozhi M, Kannabiran K, Kumar R & Khanna VG, Antifungal activity of Streptomyces sp. VITSTK7 and its synthesized Ag2O/Ag nanoparticles against medically important *Aspergillus* pathogens. *J Mycol Med*, 23 (2013) 97.
30 Chaturvedi V & Kumar A, Diversity of culturable sodium dodecyl sulfate (SDS) degrading bacteria isolated from detergent contaminated ponds situated in Varanasi city, India. *Int Biodeter Biodegr*, 65 (2011) 961.
31 Yen KM, Karl MR, Blatt LM, Simon MJ, Winter RB, Fausset PR, Lu HS, Harcourt AA & Chen KK, Cloning and characterization of a Pseudomonas mendocina KR1 gene cluster encoding toluene-4-monooxygenase. *J Bacteriol*, 173 (1991) 5315.
32 Bai H, Zhang Z, Guo Y & Jia W, Biological Synthesis of Size-Controlled Cadmium Sulfide Nanoparticles Using Immobilized *Rhodobacter sphaeroides*. *Nanoscale Res Lett*, 4 (2009) 717.
33 Dhoondia ZH & Chakraborty H, Lactobacillus mediated synthesis of silver oxide nanoparticles nanomater. *Nanotechnol*, 2 (2012) 15.
34 Kalishwaralal K, Deepak V, Pandian SRK, Kottaisamy M, BarathmaniKanth S, Kartikeyan B & Gurunathan S, Biosynthesis of silver and gold nanoparticles using *Brevibacterium casei*. *Colloids Surf B Biointerfaces*, 77 (2010) 257.
35 Vigneshwaran N, Kathe AA, Varadarajan PV, Nachane RP & Balasubramanya RH, Biomimetics of silver nanoparticles by white rot fungus, *Phaenerochaete chrysosporium*. *Colloids Surf B Biointerfaces*, 53 (2006) 55.
36 Kalimuthu K, Suresh Babu R, Venkataraman D, Bilal M & Gurunathan S, Biosynthesis of silver nanocrystals by *Bacillus licheniformis*. *Colloids Surf B Biointerfaces*. 65 (2008) 150.
37 Sneha K, Sathishkumar M, Mao J, Kwak IS & Yun YS, *Corynebacterium glutamicum*-mediated crystallization of silver ions through sorption and reduction processes. *Chem Eng J*, 16 (2010) 2989.
38 Chai Y, Chu F, Kolter R & Losick R, Bistability and biofilm formation in Bacillus subtilis. *Mol Microbiol*, 67 (2008) 254.
39 Nadell CD, Xavier JB & Foster KR, The sociobiology of biofilms. *FEMS Microbiol Rev*, 33 (2009) 206.
40 Stanley NR, Britton RA, Grossman AD & Lazazzera BA, Identification of catabolite repression as a physiological regulator of biofilm formation by *Bacillus subtilis* by use of DNA microarrays. *J Bacteriol*, 185 (2003) 1951.
41 Houry A, Briandet R, Aymerich S & Gohar M, Involvement of motility and flagella in *Bacillus cereus* biofilm formation. *Microbiology (Reading)*, 156 (2010) 1009.